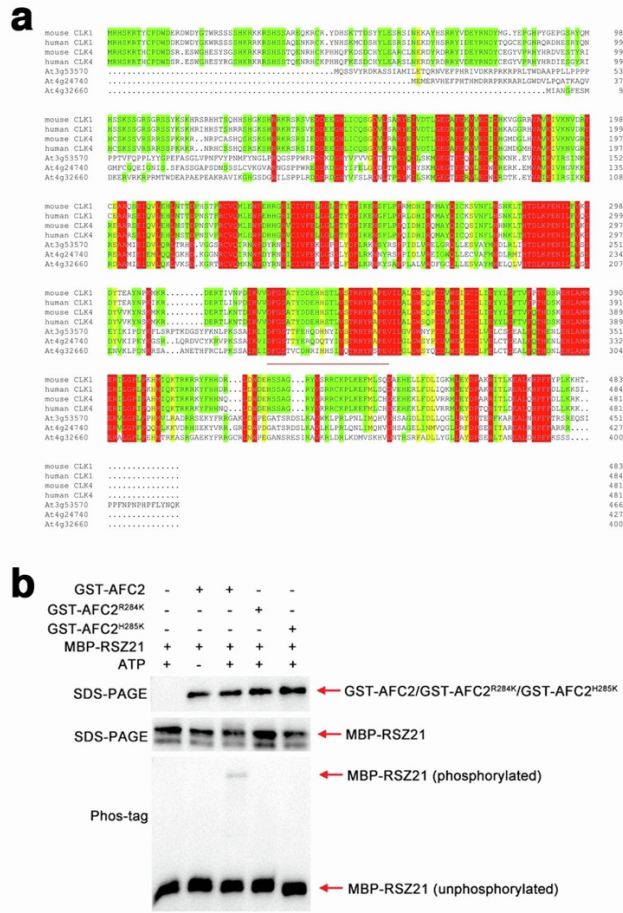


iScience, Volume 25

Supplemental information

Plant AFC2 kinase desensitizes thermomorphogenesis through modulation of alternative splicing

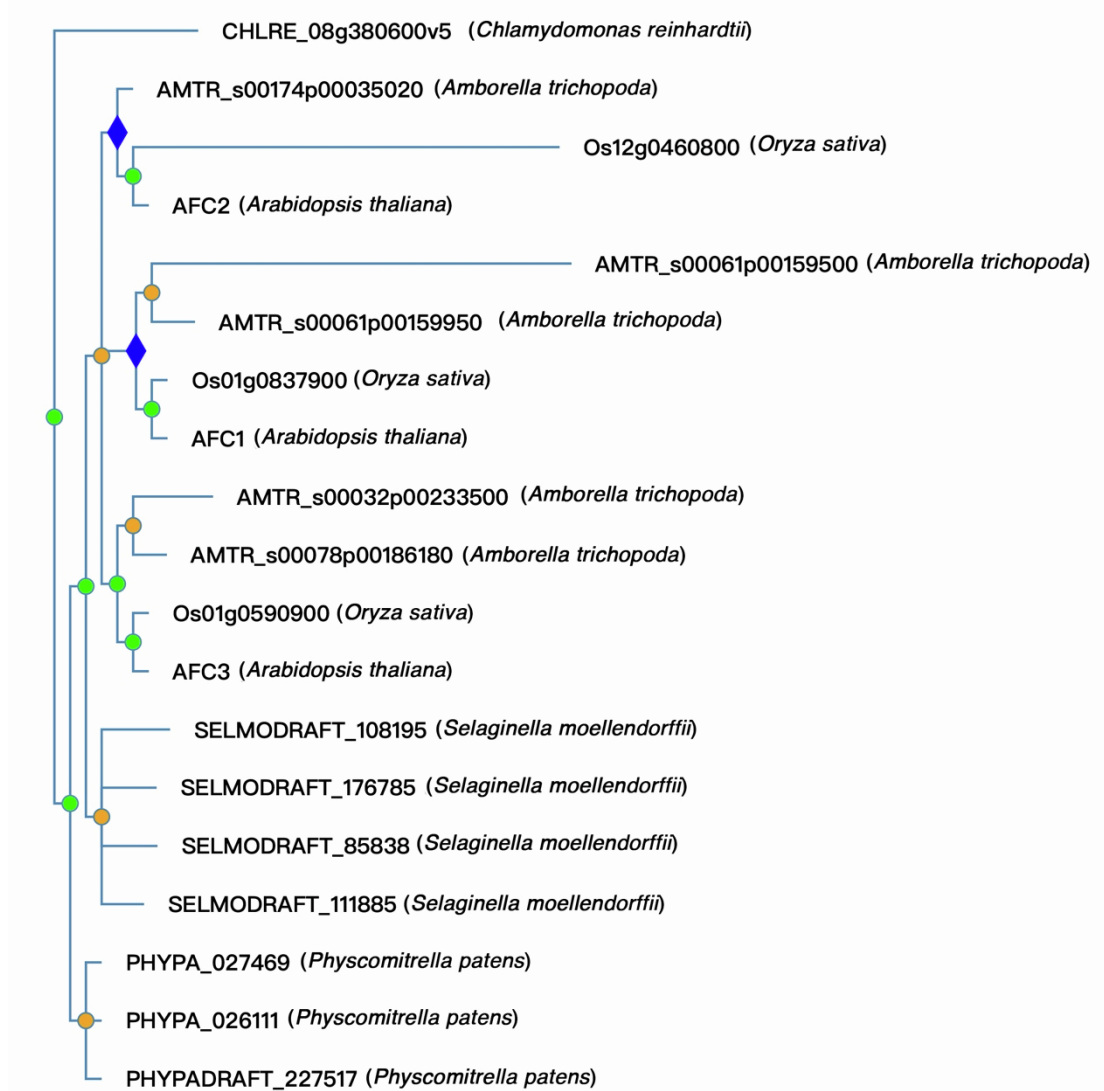
Jingya Lin, Junjie Shi, Zhenhua Zhang, Bojian Zhong, and Ziqiang Zhu



Supplementary Figure 1: AFC2 is a conserved CLK kinase in *Arabidopsis thaliana*, related to Figure 1

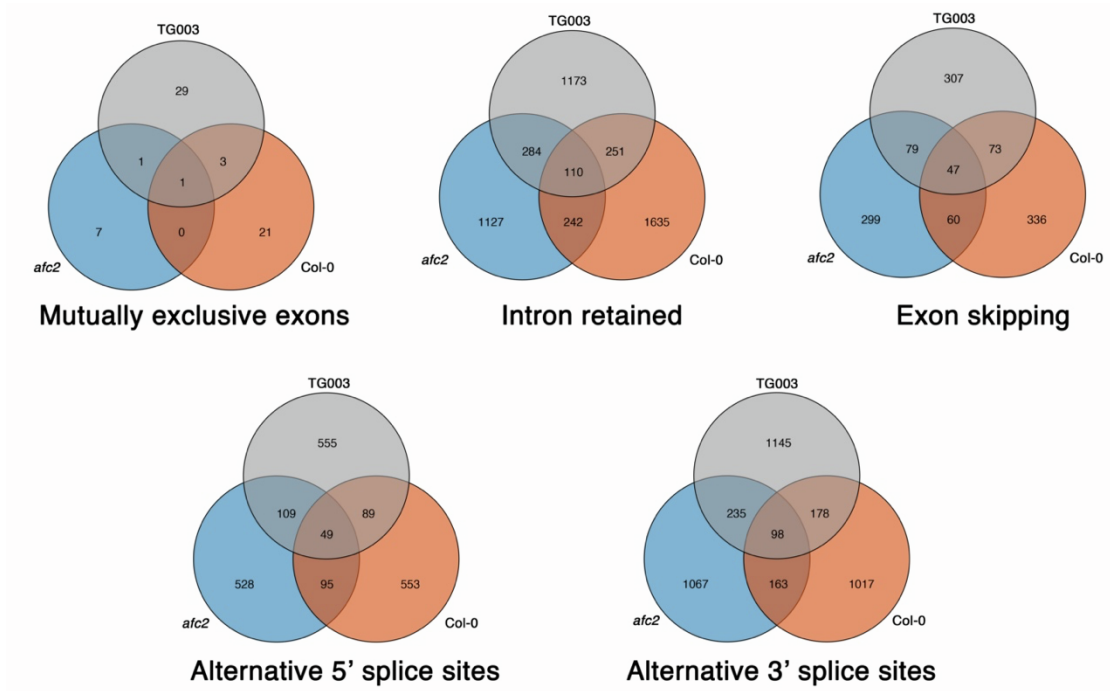
a. Amino acid sequence alignments. The amino acid sequences of mouse CLK1, human CLK1, mouse CLK4 and human CLK4 were compared with those of Arabidopsis AFC1 (At3g53570), AFC2 (At4g24740), and AFC3 (At4g32660). Red represents 100% identical amino acids, yellow represents more than 75% identical amino acids, and green represents more than 50% identical amino acids. The straight line illustrates the kinase activation segment regions.

b. AFC2 phosphorylated RSZ21. GST-fused AFC2 or mutated versions of AFC2 were incubated with MBP-RSZ21 substrates at room temperature with or without ATP for 60 min. The kinase activity was monitored with immunoblotting from Phos-tag SDS-PAGE gels, while the loading controls were detected with immunoblotting from regular SDS-PAGE gels. The shifted MBP-RSZ21 bands on the Phos-tag SDS-PAGE gel represented phosphorylated forms, while the unshifted bands indicated unphosphorylated forms. GST-fusion proteins were detected with an anti-GST antibody, while MBP-RSZ21 proteins were detected with an anti-MBP antibody.



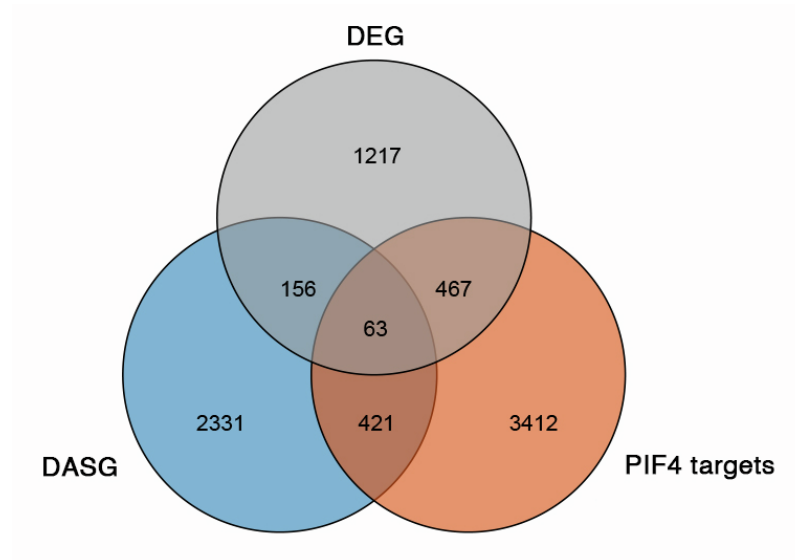
Supplementary Figure 2: AFC2 phylogenetic tree, related to Figure 1

Phylogenetic trees illustrated the relationships among the AFC members in different plant lineages.



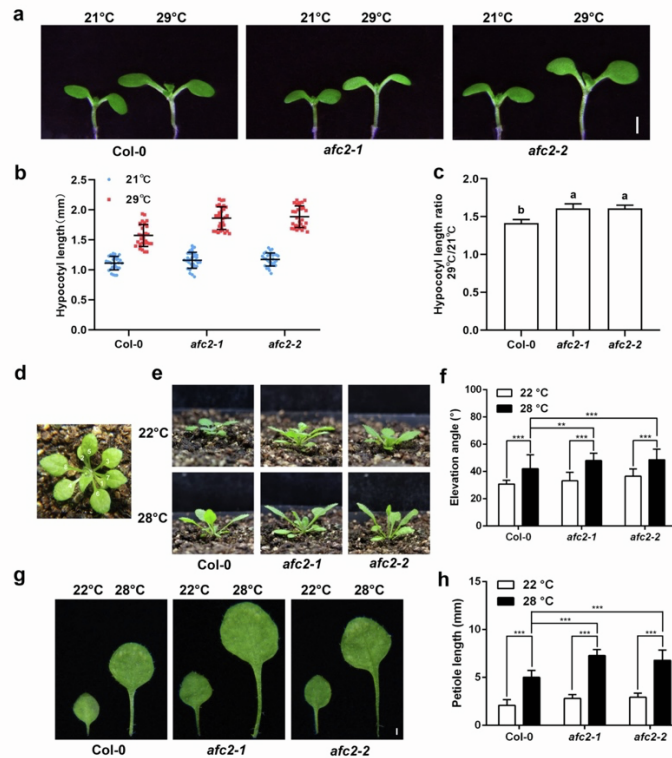
Supplementary Figure 3: Alternative splicing types, related to Figure 1

Venn diagram showing the numbers of differential alternative splicing types in all the treatments.



Supplementary Figure 4: Analyzing the exact numbers of alternative splicing events, transcriptional regulation and PIF4 binding sites, related to Figure 1

Venn diagram depicting the overlaps among differential alternative splicing (DASG), differentially expressed genes (DEGs) in Col-0 and published PIF4 binding sites (PIF4 targets).



Supplementary Figure 5: *afc2* mutants are hypersensitive to high temperature, related to Figure 2

a. Representative images showing hypocotyl phenotypes in Col-0, *afc2-1* and *afc2-2* grown at the indicated temperature. Scale bar=1 mm.

b. Quantification analysis of the hypocotyl lengths of Col-0, *afc2-1* and *afc2-2* grown at 21°C or 29°C. Data are represented as mean +/- SD. $n=30$.

c. The hypocotyl elongation ratio calculated from the results shown in (b). Significant differences are indicated by letters, $P \leq 0.01$.

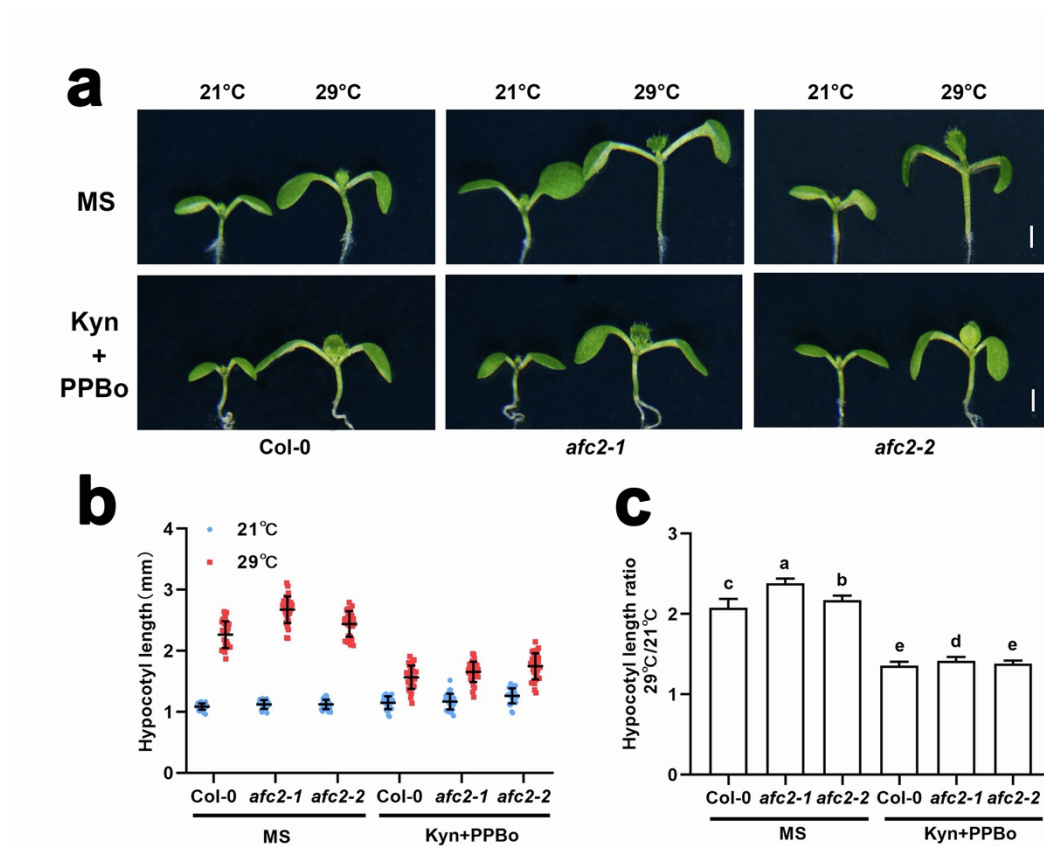
d. Diagram depicting individual leaf positions in adult plants.

e. Representative images showing the rosette leaf elevation angles in 20-day-old Col-0, *afc2-1* and *afc2-2* plants grown at the indicated temperatures.

f. Quantitative analysis of rosette leaf elevation angles in plants as described in (e). Statistical analysis was performed with a *t*-test ($**P \leq 0.05$, $***P \leq 0.01$), $n=18$.

g. Representative images showing the 5th or 6th rosette leaf petiole lengths in 20-day-old Col-0, *afc2-1* and *afc2-2* plants.

h. Quantitative analysis of petiole lengths in plants as described in (g). Statistical analysis was performed with a *t*-test ($**P \leq 0.05$, $***P \leq 0.01$), $n=18$.



Supplementary Figure 6: Auxin biosynthesis is required for *afc2* hyperresponsiveness to high temperature, related to Figure 2

a. Representative images showing hypocotyl phenotypes in plants grown on MS medium in the presence of 5 μM of Kyn and 1 μM of PPBo treatment (Kyn+PPBo) at the indicated temperature. Scale bar=1 mm.

b. Quantification analysis of hypocotyl lengths in plants grown on MS or Kyn+PPBo at the indicated temperatures. Data are represented as mean \pm SD. $n=30$.

c. The hypocotyl elongation ratio was calculated from the results shown in (b). Significant differences are indicated by letters, $P \leq 0.01$.